Control of Energy Transfer to CdTe Nanowires via Conjugated Polymer Orientation

ARTICLE *in* THE JOURNAL OF PHYSICAL CHEMISTRY C · DECEMBER 2008

Impact Factor: 4.77 · DOI: 10.1021/jp807065a

8 AUTHORS, INCLUDING:

Jaebeom Lee
Pusan National University
104 PUBLICATIONS **3,246** CITATIONS
SEE PROFILE

Jinsang Kim
University of Michigan
97 PUBLICATIONS **3,772** CITATIONS
SEE PROFILE

Kangwon Lee
Korea University
14 PUBLICATIONS **539** CITATIONS
SEE PROFILE

Nicholas Kotov
University of Michigan
445 PUBLICATIONS **27,111** CITATIONS
SEE PROFILE

Control of Energy Transfer to CdTe Nanowires via Conjugated Polymer Orientation

Jaebeom Lee,*,† Hyong-Jun Kim,▽ Ting Chen,§ Kangwon Lee,‡ Ki-Sub Kim,○ Sharon C. Glotzer,‡,§,¶,# Jinsang Kim,‡,§,¶,⊥ and Nicholas A. Kotov‡,§,⊥

Department of Physics, Chemical Engineering, Biomedical Engineering, and Material Sciences and Engineering, and Macromolecular Science and Engineering, University of Michigan, Ann Arbor, Michigan 48109, Department of Nanomedical Engineering, Pusan National University, Miryang, 627-706 Korea, and Department of Chemical and Biological Engineering, Chungju National University, Chungju 380-702

Received: August 6, 2008; Revised Manuscript Received: October 16, 2008

Nanoscale organic−inorganic hybrid materials were prepared from two highly fluorescent building blocks: CdTe nanowires (NWs) as an energy acceptor, and a rigid rod-like and water soluble poly(*p*-phenyleneethynylene) (PPE) as a donor. The PPE was covalently bonded to the CdTe by traditional amide chemistry. Two different orientations, parallel and perpendicular, of PPE to CdTe NW were achieved by manipulating the density of PPE at the NW surface through controlling the molar ratio of PPE and the NW during the chemical tethering. Strong dependence of fluorescence resonance energy transfer (FRET) on the orientation was observed. While efficient FRET was observed when the orientation of the donor PPE and the acceptor CdTe NW is parallel, essentially no FRET was observed from the perpendicularly oriented PPE-tethered CdTe NW system. Optical and transmission electron microscopy experiments as well as Monte Carlo simulation consistently suggest that entropy change during the tethering is a crucial factor for the determination of the orientation of PPE at the NW surface.

1. Introduction

Extensive studies on nanoscale composites of polymers and inorganic materials have been carried out for the design of fundamental comprehension of physicochemical phenomena in the nanoscale regime and for practical applications in optical and electronic devices and biomedical applications.[1−13]

As such, fluorescent semiconductor nanowires (NW) can lead to devices with efficient emission across the entire visible spectrum.[14−18] Among 1-D quantum structures, poly(*p*-phenyleneethynylene) (PPE) having a conjugated backbone can be described as a rigid rod-like molecules. They have been utilized for the self-assembly of 2-D molecular architectures to modulate sensory response[19−25] and for polarized photoluminescence (PL) that are suitable for use in light-emitting diodes.[26−29]

While photophysics of an individual 1-D system have been studied quite extensively, nanowire/nanorod assemblies of different geometries introduce a lot of new parameters essential both from fundamental and practical perspectives. The pathways of energy flow between different parts of the assemblies are still poorly understood. One of the key electronic interactions between nanosacle building blocks is fluorescence resonance energy transfer (FRET), used as a basis for development of sensing and actuating devices in hybrid materials.[30−36] FRET is a nonradiative dipole−dipole coupling mechanism governed to a large extent by the spectral overlap between the emission spectrum of the donor and the absorption spectrum of the acceptor, as well as by the distance between donor and acceptor.[14,15] The transfer efficiency usually taken as a measure of the distance strongly depends on the mutual orientation of the donor and acceptor emission/absorption dipoles.[37] In the 0-dimensional or multidirectional superstructures, e.g., linked nanoparticles,[38,39] the orientation factor is seldom considered and is taken to be a constant. An exception is plasmon-exciton interactions between metallic and semiconductor nanoparticles, which are somewhat similar to FRET, where the geometry of the produced nanoscale systems plays the primary role in determining their optical properties.[40−42] Several experimental and theoretical studies on polymeric systems indicate that in one-dimensional structures the orientation is also not a negligible factor; for example, the energy transfer between two dyes entangled at each end of helical DNA was dominated by the orientation.[43−50]

It was also shown that the energy transfer in block polymers also depended on the directional alignments of the polymer chain,[27,50] and moreover Palman et al. reported that synthetic modification of an optically active PPE polymer allowed for the generation of both polarized absorption and luminescence by subsequent global orientation of the nanostructure.[51] Contribution of geometry can also be seen in the 1-D hybrid (1-D) system essential for electronic and biological applications.[52−56]

All these studies give indication that the orientation factor in FRET may play a significant role in the energy transfer in nanoscale axial colloids which have some similarities with polymers. It would be interesting and fundamentally important, however, to demonstrate this experimentally using nanowires or nanorods, especially in the hybrid polymer−NW superstructures and find the methods of controlling it. This would demonstrate the generality of the geometrical effects in FRET-active one-dimensional systems and provide tools for manipulat-

* To whom correspondence should be addressed. E-mail: jaebeom@pusan.ac.kr. Phone: 82-55-350-5298. Fax: 82-55-350-5653.
† Pusan National University.
‡ Department of Materials Science and Engineering, University of Michigan.
§ Department of Chemical Engineering, University of Michigan.
¶ Department of Macromolecules Science and Engineering, University of Michigan.
⊥ Department of Biomedical Engineering, University of Michigan.
Department of Physics, University of Michigan.
○ Chungju National University.
▽ Present address: OLED center, Seoul National University, Seoul, Korea 151-744.

10.1021/jp807065a CCC: $40.75
Published on Web 12/04/2008

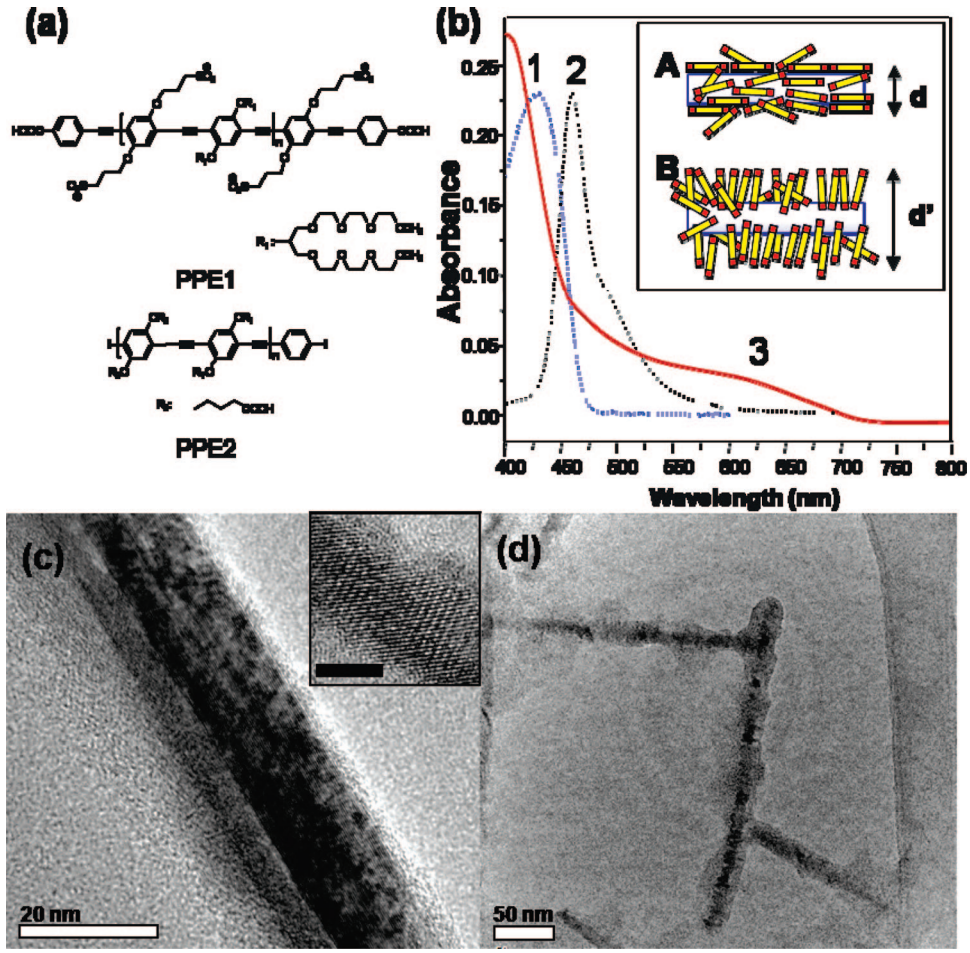

Figure 1. (a) Chemical structure of two different types of PPE polymers. (b) Optical properties of the PPE1 and CdTe NW, 1, absorbance of PPE1, 2, fluorescence of PPE1, 3, absorbance of the CdTe NW, (insert) schematics of conjugation of PPE1 and the NW, A, parallel conjugation of PPE1 and the NW, B, perpendicular conjugation of PPE1 and the NW, and TEM image of (c) NW4, (d) NW7 in Table 1.

ing energy pathways in the assembled structures. The nanoscale superstructures between polymers and semiconductor colloids offer remarkable structural variety of both types of building blocks which makes possible creation of a new family of nanoscale superstructures combining the structural and optical advantages of both classes of compound-relevant optics including negative index materials, electronics, biosensing, and solar energy conversion.[17,57−59]

In this study, we observed FRET between PPE polymer and CdTe NW, and its efficiency depends very strongly on the orientation of tethered polymers. In particular, the PPE tethered with the NW composed of alternating ionic sulfonate units and bifurcated nonionic ethylene oxide units make possible high colloidal stability in an aqueous state with high water solubility, strong fluorescence,[60,61] and structural manipulation of the inorganic/organic superstructures. Different orientation of PPE around CdTe was induced by the variation of the PPE/NW ratio during the binding stage. High density of the rigid PPE1 around the NWs forced them to acquire perpendicular orientation to the NW in a brush-like fashion, which can potentially be quite typical for assemblies of 1-D nanoscale structures.[61] Computer simulation confirmed the orientation of the building blocks and revealed that the orientation of the rod-shaped polymers on the surface of CdTe NWs is driven by the entropy of the polymer. The difference in orientation leads to marked change in the photoluminescence properties of the constructs with strong FRET in parallel orientation and no energy transfer when the orientation is perpendicular despite several times greater local concentration of FRET donor for the latter.

2. Experimental Section

The preparation of water soluble PPE polyelectrolytes was described in detail elsewhere.[60] Two different types of PPE polymers were utilized (Figure 1a). For PPE1, the molecular weight of the synthesized PPE1 was 13 000 g/mol characterized by ^{1}H NMR end-group analysis; its peak wavelength of luminescence was 470 nm with the absolute quantum yield of 53%. Both ends of PPE1 were terminated with a carboxylic group. The maximum length and hydrodynamic radius of the polymer in aqueous state was calculated as 12.13 and 2.56 nm, respectively. The molecular weight and optical properties of PPE2 were similar to that of PPE1 (simulated by Materials Studio 3.0), and the absolute quantum yield of PPE2 was 51%. CdTe NPs (nano particles) and NWs were prepared as mentioned elsewhere in detail.[62] The average diameter of cysteine-stabilized CdTe NWs is 7.2 ± 2.1 nm, the average length is 120 nm, and the peak wavelength of luminescence is 665 nm. On the basis of the structural and geometrical information, it can be calculated that the CdTe NW can accommodate about 110 molecules of PPE1 in parallel arrangement and about 520 molecules of PPE1 in the perpendicular arrangement.

To link affinity of PPE1 to CdTe NWs, both carboxylic end groups of the polymer were substituted with NHS by EDC/sulfo-NHS procedures.[63] EDC and NHS stand for 1-ethyl-3-(3-dimethlaminopropyl)carbodiimide hydrochloride and *N*-hydroxysulfosuccinimide that were purchased from Aldrich and Merck, respectively. The dried PPE polymer was diluted in deionized water (18 MΩ, Barnstead E-pure system) as the final concentra-

TABLE 1: Experimental Conditions and Molarity Ratios of PPE-Conjugated NWs Used for Superstructures and Optical Measurements

solution	NW (μL)	PPE (μL)	molarity ratio (M_{PPE}/M_{NW})
NW1	200	0	0
NW2		4	77
NW3		10	193
NW4		20	385
NW5		60	1155
NW6		500	9625
NW7		1000	19250

tion of 3.85×10^{-6} M. Fresh solutions of 0.2 M EDC (0.077 g) in 2 mL of DI water, and 25 mM NHS (0.011 g) in 2 mL of DI water, were respectively prepared at pH 6. Then 1 mL of PPE polymer solution was mixed with EDC and NHS solution with gentle stirring for 30 min, and the ultracentrifuge at 35 000 g (14 000 rpm, Beckman J2-MI) to separate NHS-substituted polymers. The precipitated polymer was redispersed in 1 mL of DI water to keep the polymer similar to the initial concentration.

CdTe NWs were tethered with this NHS-substituted polymer right after the polymer treatment. The concentration of the original solution of CdTe NW was approximated as $\sim 10^{-9}$ M that was based on used Cd or Te salts in the synthesis procedure and the geometrical information of the NPs and NWs gathered from atomic force microscopy (AFM) and transmission electron microscopy (TEM). The molarity ratios of PPE1/NW were changed through the volume change of PPE1 when the volume of the NW solution was fixed (Table 1). The PPE1-tethered NWs were centrifuged at 5000−10 000 rpm to separate free polymers, and then the precipitated NWs were redispersed in DI water (pH 9 adjusted by 1 M NaOH solution). This centrifuging and redispersion was repeated 2−3 times. Finally, the prepared samples were kept in the dark place for further optical experiments. The luminescence spectra of PPE1-tethered NW dispersions were registered with a Fluoromax-3 spectrofluorometer. Twenty microliter aliquots of the prepared samples were added to an optical cuvette of 3 mL of deionized water (pH 9) to measure the luminescence at the excitation wavelength of 420 nm. The size and surface charge of the PPE1-tethered NWs were measured by Zetasizer Nano-ZS (Malvern, United Kingdom) at multimode distribution measurement. The amount of the measured superstructure was decreased up to 10^{-16} M based on the molarity of the NW in order to avoid unwanted aggregation. The electronic images were obtained from TEM (JEOL 2010F).

3. Results and Discussion

Two types of fluorescent conjugated polymers, PPE1 and PPE2, were tested for the formation of rigid rod assemblies with NWs (Figure 1). Conjugation of PPE2 to NWs resulted in aggregation and precipitation. However, the conjugates of PPE1 and CdTe NWs were colloidally stable and afforded detailed optical studies. The difference between stability of the solutions of conjugates should be attributed to a substantially greater degree of ionization of SO_3^-groups in PPE1 than COOH groups in PPE2, and the fact that once COOH groups on the side chains of PPE2 were consumed by amide bond formation with NWs, the solubility of PPE should be lowered significantly.

The highly emissive and completely water-soluble conjugated PPE1 can be described as a rod-like molecule because of multiple carbon−carbon triple bonds and benzene rings as well as the bulky branches at each repeating unit that sterically hinder rotation or bending of the polymer. Note also that the length of the PPE1 polymer is relatively short; the maximum length is 12.13 nm in aqueous solutions compared to a few hundreds of nanometers in the cases of NWs. The carboxylic groups located exclusively at the ends of PPE1 enable further conjugation to biological or inorganic moieties with well-defined coupling chemistry (Figure 1a).[63] The optical properties of PPE1 showed the emission at 470 nm that can be thoroughly overlapped by the absorbance band of CdTe NW (Figure 1b). One can expect that most of the emission energy from PPE1 can transfer to the CdTe NW when the distance and orientation of donor and acceptor, namely, the fluorescent polymer and NW, are appropriately controlled from the fluorescence resonance energy transfer (FRET) effect (eq 1). The efficiency, E, of FRET can be described by eq 1,

$$R_o = 0.2108[J_{DA}(\lambda)K^2 n^{-4}\Phi_D]^{1/6}$$

$$E = R_o^6/[R_o^6 + R_{DA}^6] \quad (1)$$

where R_{DA} is the distance between the fluorescence donor and acceptor, and R_o is the distance (Å) at which half of the energy is transferred (the Förster radius). J_{DA} in the second equation is the donor/acceptor spectral overlap integral, and κ is a geometric factor associated with the orientation of the donor and acceptor dipoles. However, the orientation κ should be delicately considered when conjugations between two 1-D fluorophores are carried out because the characteristic of orientation is another dominant factor in the FRET effect.[64−66] The insert of Figure 1b presents examples of different polymer modes of attachment to CdTe NWs. Since PPE1 has two anchors in the respective ends of polymer backbone, two ultimate geometrical opportunities arise when it is attached to CdTe NW. One is the so-called, horizontally oriented conformation when both of the NHS-substituted carboxylic groups in the polymers reacted with the amine groups of the stabilizers of CdTe NW. The other case is perpendicularly oriented conformation when the PPE1 rods are attached to NWs by only one carboxyl group and form a centipede-like structure. Since the latter case corresponds to a much higher density of polymer molecules around the NW, one may hypothesize that the dominant geometry of the superstructure will depend on the molar ratio of both building blocks. It is assumed that one of the driving forces for a different orientation would be the packing density of the PPE1 polymer on the NW surface when other thermodynamic variants are constant. Computer simulations on polymer−nanoparticle composites reported that the conformation of polymers on the surface depended on the density of polymers in the vicinity of spherical colloids.[67−71] In more practical terms, when low PPE1 concentrations are added to a constant amount of NW, both anchors (NHS-substituted carboxylic groups) of the polymer have high probability to be tethered to the NH_2 groups of NW stabilizers and thus form the parallel structure. However, when high PPE1 concentrations are added to a constant amount of NW, the attachment of the second parallel layer might not be possible because of the densely packed environment on the surface of the NW, and thus the orientation of PPE1 will be mostly perpendicular to the NW axis.

Figure 1c,d presents TEM images of two typical samples, such as NW4 and NW7 (see Table 1) with vastly different PPE1/NW molar ratios, i.e. 385 and 19250, respectively. In the TEM image obtained for NW4 (Figure 1c), the thickness of the layer of PPE1 encapsulating the NW is less than 3 nm which corresponds to the hydrodynamic radius of PPE1 used. This suggests that the PPE1 rods are oriented parallel to the NWs.

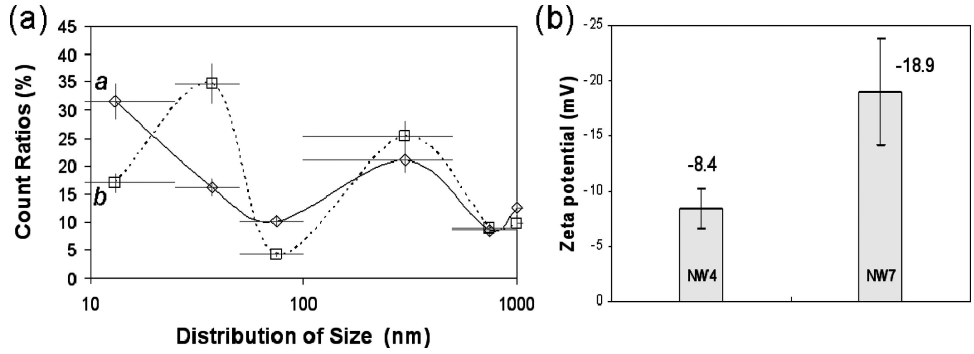

Figure 2. (a) The size distribution of PPE1-tethered CdTe NW in aqueous solution (pH 9): a, NW4, b, NW7. Each dot in the graph indicates the median point of each distribution range (X error bars), (b) the zeta potential measurement of NW4 and NW7.

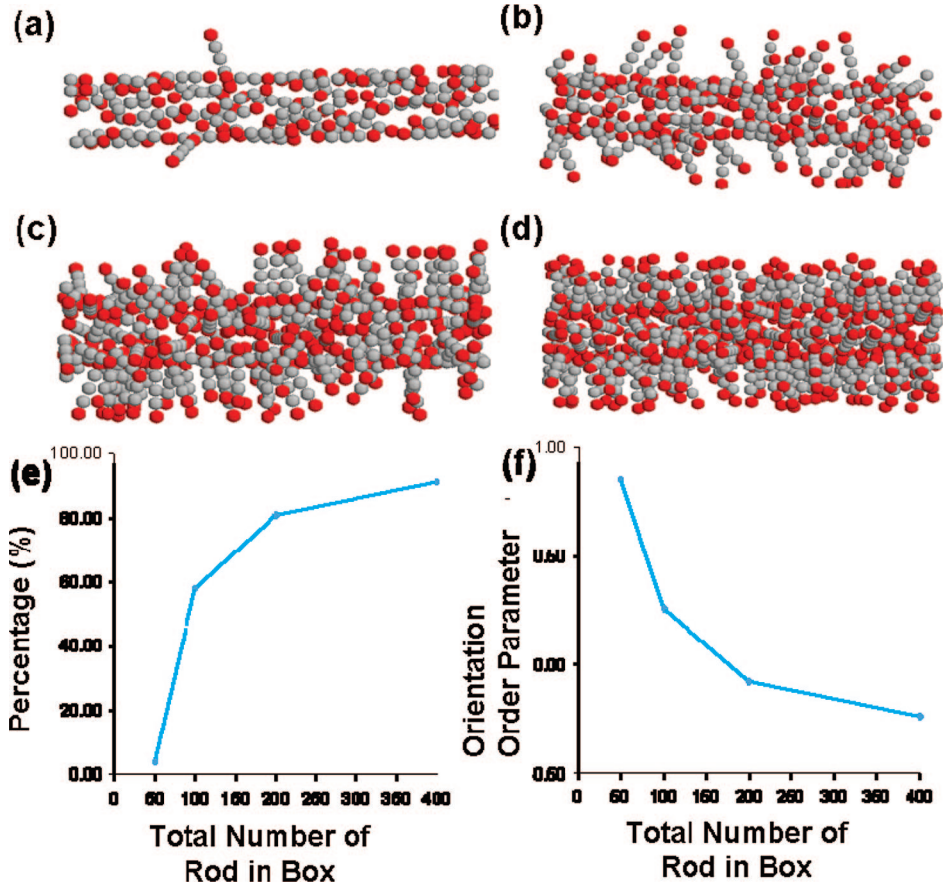

Figure 3. (a−d) Molecular simulations on a minimal model performed for a nanowire−polymer rod system with different numbers of polymer rods, $N = 50$, 100, 200, and 400, in a simulation box with a size of 30σ, as described in the text. For clarity, only polymer rods adsorbed on the NW are shown. (e) Percentage of the adsorbed polymer rods that are in perpendicular configuration. (f) The total orientation order parameter, S, as a function of the total number of rods in the simulation box.

Note again that the formation of double layers on the surface of the NW is not possible because the groups suitable for coupling chemistry would not be available in this case. The TEM image in Figure 1d describing NW7 shows that the polymer layers cover CdTe NWs with layers more than 10 nm in thickness. This thickness almost perfectly corresponds to the length of the polymer, suggesting that PPE1 is perpendicularly oriented to the surface of the NW. The details of the internal structure of NW4 can also be seen substantially better than in the opaque image of the NW7 inside the PPE1 shell because of the scattering of the irradiated electron beam in the thick organic shield from PPE1 as well as because of free-hovering electron charges of unconjugated polymer headgroups.

TEM images show the geometry of the superstructure in the dry state. It is useful to obtain a corroborating piece of evidence of the parallel and perpendicular arrangements in the aqueous state. Hence, we utilized dynamic light scattering (DLS) using Zetasizer (Malvern, Nano-ZS) that can access bimodal size distribution, e.g., hydrodynamic longitudinal and horizontal dimensions of NW−polymer structures in the aqueous state. All particle-sizing techniques such as DLS have an inherent problem in describing the size of nonspherical particles because the hydrodynamic diameter of a nonspherical particle is the diameter of a sphere that has the same translational diffusion speed as the spherical particle. If the shape of a particle, however, changes in a way that affects the diffusion speed, then the hydrodynamic size will change. As the changes will usually affect the diffusion speed and the DLS is a very sensitive technique for detecting these changes, it would be possible to distinguish the longitudinal and horizontal dimension in large

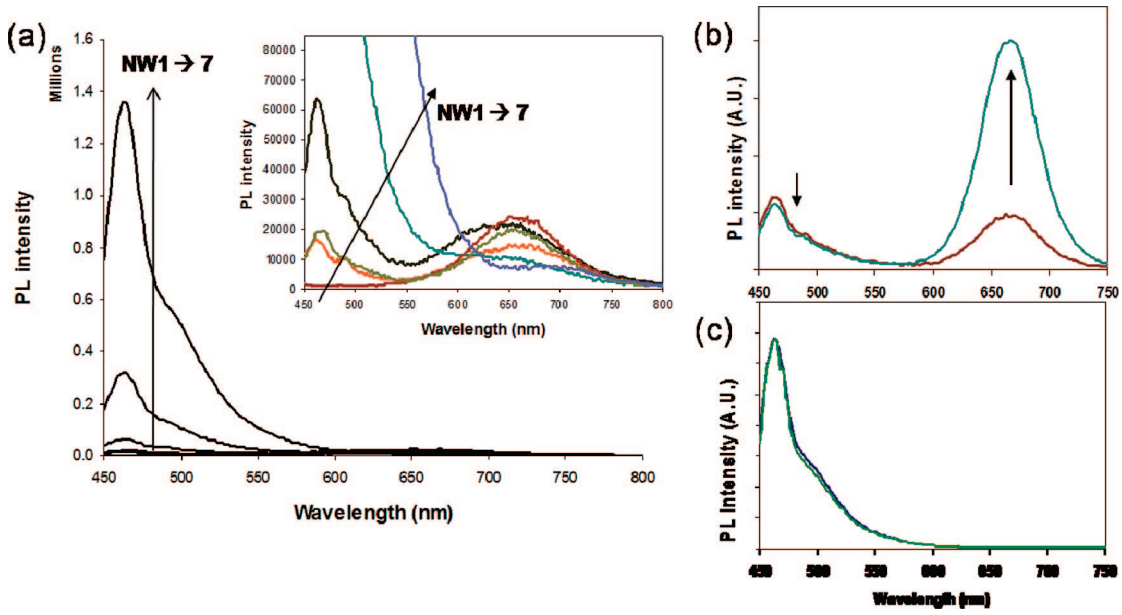

Figure 4. (a) Fluorescence emission spectra of NW1−7: excitation wavelength was at 420 nm. Insert: Fluorescence emission spectra of NW1−7 in the low intensity in order to show the NW intensities. (b and c) Fluorescence emission spectra revealing differences in FRET in NW4 and NW7, respectively, excitation wavelength was at 420 nm.

TABLE 2: Enhancement Ratios of the PPE1-Tethered NWs[a]

solution	I_{FRET}/ I_{PPE1}	I_{FRET}/I_{NW}
NW1	n/a	n/a
NW2	0.98	1.05
NW3	0.96	1.40
NW4	0.91	4.20
NW5	0.68	2.20
NW6	1.03	1.02
NW7	1.00	1.00

[a] I_{FRET} is the luminescence intensity of the NW after FRET reaction and I_{NW} (or I_{PPE}) is the initial luminescence intensity of the NW (or PPE).

variation. In particular, since the aspect ratio of the prepared NW is approximately more than several hundred, two distinguishable bands could be observed at each graph of NW4 and NW7, i.e., 1−50 nm for the diameter and 100−1000 nm for the longitudinal length (Figure 2a). Notice that two samples presented opposite diameter distributions at the range of 1−50 nm, i.e., the major size distribution of NW4 resided at 1−25 nm while that of NW7 was located at 25−50 nm. One can clearly notice that the diameter of NW7 was thicker than that of NW4 in the aqueous state. The zeta potential of the superstructure of NW4 and NW7 in pH 9 aqueous solution provides an additional, although circumstantial, piece of evidence in support of parallel and perpendicular orientations of PPE1. NW7 has a much higher zeta potential than NW4 (Figure 2b). Since the surface charge comes from the ionization of the stabilizers of NWs and the SO_3^- functional groups of PPE1, the stronger negative charge in NW7 correlates very well with the greater density of PPE1 in perpendicular arrangement.

Altogether, these results demonstrate that the orientation of rigid polymers can be ultimately manipulated through molecular engineering of packing density and steric/geometric hindrance.[72] Further proof of the geometrical differences between NW4 and NW7 can be obtained by computer modeling, which also can help us to reveal the driving force of the orientational change. Monte Carlo simulations on a minimal model were performed for the NW−polymer rod system. The length unit in the minimal model is $\sigma = 2.5$ nm. The polymer rod is modeled as five beads fused tangentially and rigidly into a linear array, giving a total length of 5σ, or 12.5 nm, and a diameter of 1σ, or 2.5 nm. Correspondingly, the NW is 50−80 σ, or 125−200 nm in length and 3−4 σ, or 7.5−10 nm in diameter. Detailed simulation conditions can be found in Supporting Information. The simulations show that at low concentration, most of the polymer rods that adsorbed onto the NW surface adopt a flat or parallel configuration in which both ends interact directly with the NW (e.g., more than 96% lying flat for $N = 50$ system) and have almost the same orientation as that of the NWs, as shown in Figure 3a. With increasing concentration, more and more adsorbed polymer rods adopt a perpendicular configuration to allow more rod ends to be in contact with the NW as shown in Figure 3b−d. Figure 3e shows the percentage of adsorbed polymer rods in the perpendicular configuration as a function of the total number of rods in the simulation box. At high concentration, almost all the adsorbed polymer rods adopt the perpendicular configuration (about 90% for $N = 400$ system), as shown in Figure 3d. Besides visual inspection of the simulation data and microscopy and light scattering data above, the observations of ordering can also be confirmed and quantified by calculation of the orientational order parameter S, i.e. the average of the second Legendre polynomial, for the polymers adsorbed with both ends and with only one end on the NW surface.[73−76]

$$S = \langle P_2(\cos\theta)\rangle = \left\langle \frac{3\cos^2\theta - 1}{2} \right\rangle$$

where θ is the angle between the rod and the "preferred direction", which is aligned with the long axis of the NW. $S = 0$ for randomly distributed rods, $S = 1$ for perfectly parallel rods, and $S = -0.5$ for perfectly perpendicular rods. As expected, even for the limiting cases, $N = 50$ and $N = 400$, which have a total orientational order parameter of 0.877 and −0.21, respectively. The orientation of polymer rods is not perfectly parallel with the NW or perfectly perpendicular to the NW (Figure 3f). The transition from the parallel configuration to the perpendicular configuration with the increasing concentra-

tion of polymers rods arises because of a competition between energy and entropy in an attempt to minimize the system free energy. The parallel arrangement is preferred energetically at all densities, while the perpendicular arrangement is preferred entropically at sufficiently high densities that packing constraints prevent all rods from contacting with the NW. By aligning themselves perpendicularly to the NW axis, albeit only at one rod end, more rods can make contact with the NW while increasing orientational freedom and thus overall entropy.

Microscopy images, data on the hydrodynamic diameter, the zeta-potential, and the Monte-Carlo simulation demonstrate that orientation of polymer rods on the surface of CdTe NWs can be controlled by the concentration of PPE1 during the stage of bioconjugation. Optical spectrometric experiments were carried out to investigate how the structure of nanoscale assemblies and the geometry of building block arrangements affect optical properties. FRET has three important factors for energy transfer from donors to acceptors: distance, spectral overlap integral, and orientation (eq 1). Considering the optical experiments involving PPE1 and CdTe NW, one needs to make the following point: the distance, R_{DA}, and spectral overlap integral, J_{DA}, can be assumed to be constant because the polymer and NW were linked by a very short amide bond and the emission band of the polymer was totally overlapped by the absorbance band of CdTe NW (Figure 1b). So, the observed optical effects, such as differences in FRET, should be attributed to the orientation change. Figure 4a shows the fluorescence spectra of the PPE1-tethered NWs depending on molarity ratios, as shown in Table 1. The inserted table presents representative values of luminescence intensity of the prepared samples and their luminescence ratios of PPE1/NW. These spectra were obtained for samples with different PPE1/NW ratios and carefully centrifuged to separate only PPE1−NW assemblies.

The results in Figure 4b and 4c show that the PL intensity of the PPE1-tethered NW was enhanced up to 4.2 times while the PL intensity of the conjugated PPE1 polyelectrolyte was slightly decreased. These are the spectral signatures of FRET, and it occurs because of alignment of dipoles in both building blocks. The favorable geometry is also complemented by strong overlap of PPE1 adsorption and CdTe emission and thus excellent resonant coupling. On the contrary, the luminescence of CdTe in NW7 did not change at all in the same experiments despite the fact that overlap of adsorption and emission is still the same. Moreover, there is at least several times greater number of PPE1 residing on each individual NW for the case of perpendicular arrangement as opposed to the parallel orientation. One can also see that FRET strength progressively decreases from NW2 to NW7 (Table 2). It is evident that the geometry of PPE1−NW assemblies strongly affects energy transfer efficiency, which must be attributed to very inefficient resonant coupling for perpendicularly aligned oscillators regardless of other favorable conditions.

In conclusion, we observed strong dependence of FRET on the arrangement of rod-type PPE1 as a donor and CdTe NWs as an acceptor in the PPE1-tethered CdTe NW system. The orientation of PPE1 was manipulated by its packing density on the surface of NWs when PPE1 and NWs were covalently bonded in an aqueous solution. Efficient fluorescence resonance energy transfer was observed when the orientation of the donor PPE1 and the acceptor CdTe NW is parallel, while essentially no FRET was observed in the perpendicularly oriented PPE1-tethered CdTe NW system. This result can be readily applicable to other organic−inorganic hybrid emissive material designs for nanoscale electronic, optical, energy harvesting, and sensory devices.

Acknowledgment. J.L. gratefully acknowledges the support of the Ministry of Information & Communications, Republic of Korea, under the Information Technology Research Center (ITRC) Support Program. N.A.K. thanks NSF and AFOSR for the support of this research. S.C.G. acknowledges funding by the National Science Foundation under CTS-0403633. J.K. thanks the NSF Career grant (DMR 0644864). J.K. acknowledges Air Force Office of Scientific Research program (FA9550-06-1-0279).

Supporting Information Available: Detailed description of the MC simulations on a minimal model for the nanowire–polymer rod system as well as diffraction results of NW–PPE superstructures. This material is available free of charge via the Internet at http://pubs.acs.org.

References and Notes

(1) Hennequin, Y.; Aarts, D. G. A. L.; Indekeu, J. O.; Lekkerkerker, H. N. W.; Bonn, D. Fluctuation Forces and Wetting Layers in Colloid-Polymer Mixtures. *Phys. Rev. Lett.* **2008**, *100* (17), 178305-1–178305-4.

(2) Kashiwagi, T.; Du, F.; Douglas, J. F.; Winey, K. I.; Harris, R. H.; Shields, J. R. Nanoparticle networks reduce the flammability of polymer nanocomposites. *Nat. Mater.* **2005**, *4* (12), 928–933.

(3) Hemmer, P. C.; Marthinsen, T. H. Phase transitions in binary mixtures of rodlike colloids and stiff polymers. *Mol. Phys.* **2002**, *100* (5), 667–671.

(4) Shenhar, R.; Norsten, T. B.; Rotello, V. M. Polymer-mediated nanoparticle assembly: structural control and applications. *Adv. Mater. (Weinheim, Germany)* **2005**, *17* (6), 657–669.

(5) Zhang, H.; Hussain, I.; Brust, M.; Butler, M. F.; Rannard, S. P.; Cooper, A. I. Aligned two- and three-dimensional structures by directional freezing of polymers and nanoparticles. *Nat. Mater.* **2005**, *4* (10), 787–793.

(6) Karthikeyan, B.; Anija, M.; Philip, R. In situ synthesis and nonlinear optical properties of Au: Ag nanocomposite polymer films. *Appl. Phys. Lett.* **2006**, *88* (5), 053104/1–053104/3.

(7) van der Beek, A. V.; Petukhov, P.; Davidson, J.; Ferr, J. P.; Jamet, H. H.; Wensink, G. J.; Vroege, W.; Bras, H. N. W. Lekkerkerker Magnetic-field-induced orientational order in the isotropic phase of hard colloidal platelets. *Phys. Rev. E: Stat., Nonlinear, Soft Matter Phys.* **2006**, *73* (4), 041402/1–041402/10.

(8) Aarts, D. G. A. L.; Lekkerkerker, H. N. W. Confocal scanning laser microscopy on fluid-fluid demixing colloid-polymer mixtures. *J. Phys. Condens. Matter* **2004**, *16* (38), S4231–S4242.

(9) Haryono, A.; Binder, W. H. Controlled arrangement of nanoparticle arrays in block-copolymer domains. *Small* **2006**, *2* (5), 600–611.

(10) Barbara, P. F.; Chang, W.-S.; Link, S.; Scholes, G. D.; Yethiraj, A. Structure and Dynamics of Conjugated Polymers in Liquid Crystalline Solvents. *Annu. Rev. Phys. Chem.* **2007**, *58*, 565–584.

(11) Flory, P. J.; Abe, A. Statistical Thermodynamics of Mixtures of Rodlike Particles. 1. Theory for Polydisperse Systems. *Macromolecules* **1978**, *11* (6), 1119–1122.

(12) Gass, J.; Poddar, P.; Almand, J.; Srinath, S.; Srikanth, H. Superparamagnetic polymer nanocomposites with uniform Fe3O4 nanoparticle dispersions. *Adv. Funct. Mater.* **2006**, *16* (1), 71–75.

(13) Corbierre, M. K.; Cameron, N. S.; Sutton, M.; Laaziri, K.; Lennox, R. B. Gold Nanoparticle/Polymer Nanocomposites: Dispersion of Nanoparticles as a Function of Capping Agent Molecular Weight and Grafting Density. *Langmuir* **2005**, *21* (13), 6063–6072.

(14) Lee, J.; Govorov, A. O.; Dulka, J.; Kotov, N. A. Bioconjugates of CdTe Nanowires and Au Nanoparticles: Plasmon-Exciton Interactions, Luminescence Enhancement, and Collective Effects. *Nano Lett.* **2004**, *4* (12), 2323–2330.

(15) Lee, J.; Govorov, A. O.; Kotov, N. A. Bioconjugated Superstructures of CdTe Nanowires and Nanoparticles: Multistep Cascade Foerster Resonance Energy Transfer and Energy Channeling. *Nano Lett.* **2005**, *5* (10), 2063–2069.

(16) Tang, Z.; Kotov, N. A.; Giersig, M. Spontaneous organization of single CdTe nanoparticles into luminescent nanowires. *Science* **2002**, *297* (5579), 237–240.

(17) Kotov, N.; Tang, Z. Organization of nanoparticles and nanowires in electronic devices: challenges, methods, and perspectives. *Nanopart. Assemb. Superstruct.* **2006**, 3–73.

(18) Wang, Y.; Tang, Z.; Tan, S.; Kotov, N. A. Biological Assembly of Nanocircuit Prototypes from Protein-Modified CdTe Nanowires. *Nano Lett.* **2005**, *5* (2), 243–248.

(19) Xu, K.; Wang, Y.; Bai, R.; Lu, W.; Pan, C. Synthesis of amphiphilic rod-coil ABC tri block copolymers with oligo(para-phenyleneethynylene) as the middle rigid block. *Polymer* **2005**, *46* (18), 7572–7577.

(20) Samori, P.; Francke, V.; Mullen, K.; Rabe, J. P. Self-assembly of a conjugated polymer: from molecular rods to a nanoribbon architecture with molecular dimensions. *Chem.—Eur. J.* **1999**, *5* (8), 2312–2317.

(21) Kim, I. B.; Bunz, U. H. F. Modulating the Sensory Response of a Conjugated Polymer by Proteins: An Agglutination Assay for Mercury Ions in Water. *J. Am. Chem. Soc.* **2006**, *128* (9), 2818–2819.

(22) Erdogan, B.; Song, L.; Wilson, J. N.; Park, J. O.; Srinivasarao, M.; Bunz Uwe, H. F. Permanent bubble arrays from a cross-linked poly(*p*-phenyleneethynylene): picoliter holes without microfabrication. *J. Am. Chem. Soc.* **2004**, *126* (12), 3678–3679.

(23) Khan, A.; Muller, S.; Hecht, S. Practical synthesis of an amphiphilic, non-ionic poly(para-phenyleneethynylene) derivative with a remarkable quantum yield in water. *Chem. Commun. (Cambridge, U. K.)* **2005**, (5), 584–586.

(24) Song, L.; Bly, R. K.; Wilson, J. N.; Bakbak, S.; Park, J. O.; Srinivasarao, M.; Bunz, U. H. F. Facile microstructuring of organic semiconducting polymers by the breath figure method: Hexagonally ordered bubble arrays in rigid-rod polymers. *Adv. Mater. (Weinheim, Germany)* **2004**, *16* (2), 115–118.

(25) Kloepfer, J. A.; Cohen, N.; Nadeau, J. L. FRET between CdSe Quantum Dots in Lipid Vesicles and Water- and Lipid-soluble Dyes. *J. Phys. Chem. B* **2004**, *108* (44), 17042–17049.

(26) Westenhoff, S.; Kotov, N. A. Quantum dot on a rope. *J. Am. Chem. Soc.* **2002**, *124* (11), 2448–2449.

(27) Hubner, C. G.; Ksenofontov, V.; Nolde, F.; Mullen, K.; Basche, T. Three-dimensional orientational colocalization of individual donor-acceptor pairs. *J. Chem. Phys.* **2004**, *120* (23), 10867–10870.

(28) Breen, C. A.; Deng, T.; Breiner, T.; Thomas, E. L.; Swager, T. M. Polarized Photoluminescence from Poly(p-phenylene-ethynylene) via a Block Copolymer Nanotemplate. *J. Am. Chem. Soc.* **2003**, *125* (33), 9942–9943.

(29) Nagasaki, Y.; Ishii, T.; Sunaga, Y.; Watanabe, Y.; Otsuka, H.; Kataoka, K. Novel molecular recognition via fluorescent resonance energy transfer using a biotin-PEG/polyamine stabilized CdS quantum dot. *Langmuir* **2004**, *20* (15), 6396–6400.

(30) Solomeshch, O.; Kigel, A.; Saschiuk, A.; Medvedev, V.; Aharoni, A.; Razin, A.; Eichen, Y.; Banin, U.; Lifshitz, E.; Tessler, N. Optoelectronic properties of polymer-nanocrystal composites active at near-infrared wavelengths. *J. Appl. Phys.* **2005**, *98* (7), 074310/1–074310/6.

(31) Bakueva, L.; Musikhin, S.; Hines, M. A.; Chang, T.-W. F.; Tzolov, M.; Scholes, G. D.; Sargent, E. H. Size-tunable infrared (1000−1600 nm) electroluminescence from PbS quantum-dot nanocrystals in a semiconducting polymer. *Appl. Phys. Lett.* **2003**, *82* (17), 2895–2897.

(32) Potapova, I.; Mruk, R.; Huebner, C.; Zentel, R.; Basche, T.; Mews, A. CdSe/ZnS nanocrystals with dye-functionalized polymer ligands containing many anchor groups. *Angew. Chem., Int. Ed.* **2005**, *44* (16), 2437–2440.

(33) Hong, S. K. Energy transfer by resonant dipole-dipole interaction from a conjugated polymer to a quantum-dot. *Phys. E (Amsterdam, Netherlands)* **2005**, *28* (1), 66–75.

(34) Warner, J. H.; Watt, A. R.; Thomsen, E.; Heckenberg, N.; Meredith, P.; Rubinsztein-Dunlop, H. Energy Transfer Dynamics of Nanocrystal-Polymer Composites. *J. Phys. Chem. B* **2005**, *109* (18), 9001–9005.

(35) Milliron, D. J.; Alivisatos, A. P.; Pitois, C.; Edder, C.; Frechet, J. M. J. Electroactive surfactant designed to mediate electron transfer between CdSe nanocrystals and organic semiconductors. *Adv. Mater. (Weinheim, Germany)* **2003**, *15* (1), 58–61.

(36) Pientka, M.; Dyakonov, V.; Meissner, D.; Rogach, A.; Talapin, D.; Weller, H.; Lutsen, L.; Vanderzande, D. Photoinduced charge transfer in composites of conjugated polymers and semiconductor nanocrystals. *Nanotechnology* **2004**, *15* (1), 163–170.

(37) Carbonnier, B.; Egbe, D. A. M.; Birckner, E.; Grummt, U. W.; Pakula, T. Correlation between Chain Packing and Photoluminescence for PPV/PPE in Macroscopically Oriented State: Side Chain Effects. *Macromolecules* **2005**, *38* (18), 7546–7554.

(38) Wang, S.; Mamedova, N.; Kotov, N. A.; Chen, W.; Studer, J. Antigen/antibody immunocomplex from CdTe nanoparticle bioconjugates. *Nano Lett.* **2002**, *2* (8), 817–822.

(39) Mamedova, N. N.; Kotov, N. A.; Rogach, A. L.; Studer, J. Albumin-CdTe Nanoparticle Bioconjugates: Preparation, Structure, and Interunit Energy Transfer with Antenna Effect. *Nano Lett.* **2001**, *1* (6), 281–286.

(40) Dulkeith, E.; Morteani, A. C.; Niedereichholz, T.; Klar, T. A.; Feldmann, J.; Levi, S. A.; van Veggel, F. C. J. M.; Reinhoudt, D. N.; Moller, M.; Gittins, D. I. Fluorescence Quenching of Dye Molecules near Gold Nanoparticles: Radiative and Nonradiative Effects. *Phys. Rev. Lett.* **2002**, *89* (20), 203002.

(41) Franzl, T.; Shavel, A.; Rogach, A. L.; Gaponik, N.; Klar, T. A.; Eychmueller, A.; Feldmann, J. High-rate unidirectional energy transfer in directly assembled CdTe nanocrystal bilayers. *Small* **2005**, *1* (4), 392–395.

(42) Govorov, A. O.; Bryant, G. W.; Zhang, W.; Skeini, T.; Lee, J.; Kotov, N. A.; Slocik, J. M.; Naik, R. R. Exciton-Plasmon Interaction and Hybrid Excitons in Semiconductor-Metal Nanoparticle Assemblies. *Nano Lett.* **2006**, *6* (5), 984–994.

(43) Lewis, F. D.; Zhang, L.; Zuo, X. Orientation Control of Fluorescence Resonance Energy Transfer Using DNA as a Helical Scaffold. *J. Am. Chem. Soc.* **2005**, *127* (28), 10002–10003.

(44) Hennebicq, E.; Pourtois, G.; Scholes, G. D.; Herz, L. M.; Russell, D. M.; Silva, C.; Setayesh, S.; Grimsdale, A. C.; Muellen, K.; Bredas, J.-L.; Beljonne, D. Exciton Migration in Rigid-Rod Conjugated Polymers: An Improved Foerster Model. *J. Am. Chem. Soc.* **2005**, *127* (13), 4744–4762.

(45) Bacchiocchi, C.; Zannoni, C. Energy transfer in condensed systems. The effect of phase organization. *Chem. Phys. Lett.* **1997**, *268* (5−6), 541–548.

(46) Bacchiocchi, C.; Brunelli, M.; Zannoni, C. Energy transfer and orientational dynamics in isotropic and nematic phases. A computer simulation approach. *Chem. Phys. Lett.* **2001**, *336* (3−4), 253–261.

(47) Kawai, T.; Yoshihara, S.; Iwata, Y.; Fukaminato, T.; Irie, M. Anisotropic translational diffusion of single fluorescent perylene molecules in a nematic liquid crystal. *ChemPhysChem* **2004**, *5* (10), 1606–1609.

(48) Zannoni, C. A theory of time dependent fluorescence depolarization in liquid crystals. *Mol. Phys.* **1979**, *38* (6), 1813–1827.

(49) Arcioni, A.; Tarroni, R.; Zannoni, C. A theory of fluorescence depolarization in mesophases with tilted distribution of directors. *Chem. Phys. Lett.* **2002**, *365* (1−2), 8–14.

(50) Jares-Erijman, E. A.; Jovin, T. M. Determination of DNA helical handedness by fluorescence resonance energy transfer. *J. Mol. Biol.* **1996**, *257* (3), 597–617.

(51) Palmans, A. R. A.; Smith, P.; Weder, C. Polarizing Energy Transfer in Photoluminescent Conjugated Polymers with Covalently Attached Sensitizers. *Macromolecules* **1999**, *32* (14), 4677–4685.

(52) Dujardin, E.; Peet, C.; Stubbs, G.; Culver, J. N.; Mann, S. Organization of Metallic Nanoparticles Using Tobacco Mosaic Virus Templates. *Nano Lett.* **2003**, *3* (3), 413–417.

(53) Ito, T.; Yamaguchi, H.; Oka, K.; Nozawa, K.; Takagi, H. Magnetism in La82xSrxCu8O20: A hybrid system with localized one-dimensional Cu-O chains and an itinerant three-dimensional Cu-O network. *Phys. Rev. B: Condens. Matter Mater. Phys.* **1999**, *60* (22), R15031–R15034.

(54) Asai, Y.; Fukuyama, H. Theory of length-dependent conductance in one-dimensional chains. *Phys. Rev. B: Condens. Matter Mater. Phys.* **2005**, *72* (8), 085431−1–085431/14.

(55) Artyukhin, A. B.; Shestakov, A.; Harper, J.; Bakajin, O.; Stroeve, P.; Noy, A. Functional one-dimensional lipid bilayers on carbon nanotube templates. *J. Am. Chem. Soc.* **2005**, *127* (20), 7538–7542.

(56) Huang, X.; Li, J.; Zhang, Y.; Mascarenhas, A. From 1D Chain to 3D Network: Tuning Hybrid II-VI Nanostructures and Their Optical Properties. *J. Am. Chem. Soc.* **2003**, *125* (23), 7049–7055.

(57) Smith, D. R.; Vier, D. C. Design of metamaterials with negative refractive index. *Proc. SPIE—Int. Soc. Opt. Eng.* **2004**, *5359*, 52–63, Quantum Sensing and Nanophotonic Devices.

(58) Patolsky, F.; Lieber, C. M. Nanowire nanosensors. *Mater. Today (Oxford, U. K.)* **2005**, *8* (4), 20–28.

(59) Beek, W. J.E.; Wienk, M. M.; Janssen, R. A. J. Efficient hybrid solar cells from zinc oxide nanoparticles and a conjugated polymer. *Adv. Mater. (Weinheim, Germany)* **2004**, *16* (12), 1009–1013.

(60) Lee, K.; Cho, J. C.; DeHeck, J.; Kim, J. Synthesis and functionalization of a highly fluorescent and completely water-soluble poly(para-phenyleneethynylene) copolymer for bioconjugation. *Chemical Commun. (Cambridge, U. K.)* **2006**, *18*, 1983–1985.

(61) Wang, Y.; Tang, Z.; Liang, X.; Liz-Marzan, L. M.; Kotov, N. A. SiO2-coated CdTe nanowires: bristled nano centipedes. *Nano Lett.* **2004**, *4* (2), 225–231.

(62) Tang, Z.; Kotov, N. A.; Giersig, M. Spontaneous organization of single CdTe nanoparticles into luminescent nanowires. *Science* **2002**, *297* (5579), 237–240.

(63) Hermanson, G. T., Ed. Bioconjugate Techniques; 1995.

(64) Ma, Y.-Z.; Miller, R. A.; Fleming, G. R.; Francis, M. B. Energy Transfer Dynamics in Light-Harvesting Assemblies Templated by the Tobacco Mosaic Virus Coat Protein. *J. Phys. Chem. B* **2008**, *112* (22), 6887–6892.

(65) Mayilo, S.; Hihorst, J.; Susha, A. S.; Hoehl, C.; Franzl, T.; Klar, T.; Rogach, A. L.; Feldmann, J. Energy Transfer in Solution-Based Clusters of CdTe Nanocrystals Electrostatically Bound by Calcium Ions. *J. Phys. Chem. C* **2008**, *112* (37), 14589–14594.

(66) Hernandez-Martinez-Pedro, L.; Govorov, A. O. Exciton energy transfer between nanoparticles and nanowires. *Phys. Rev. B: Condens. Matter Mater. Phys.* **2008**, *78* (3), 035314−1035314−7.

(67) Zhao, L.; Li, Y. G.; Zhong, C.; Mi, J. Structure and effective interactions in polymer nanocomposite melts: an integral equation theory study. *J. Chem. Phys.* **2006**, *124* (14), 144913−1144913−8.

(68) Hooper, J. B.; Schweizer, K. S. Contact Aggregation, Bridging, and Steric Stabilization in Dense Polymer-Particle Mixtures. *Macromolecules* **2005**, *38* (21), 8858–8869.

(69) Starr, F. W.; Schroder, T. B.; Glotzer, S. C. Molecular dynamics simulation of a polymer melt with a nanoscopic particle. *Macromolecules* **2002**, *35* (11), 4481–4492.

(70) Doxastakis, M.; Chen, Y. L.; Guzman, O.; De Pablo, J. J. Polymer-particle mixtures: Depletion and packing effects. *J. Chem. Phys.* **2004**, *120* (19), 9335–9342.

(71) Papakonstantopoulos, G. J.; Yoshimoto, K.; Doxastakis, M.; Nealey, P. F.; de Pablo, J. J. Local mechanical properties of polymeric nanocomposites. *Phys. Rev. E: Stat., Nonlinear, Soft Matter Phys.* **2005**, *72* (3−1), 031801/1–031801/6.

(72) Mark, A.; Horsch Zhenli, Z.; Sharon, C. Glotzer Self-assembly of polymer-tethered nanorods. *Phys. Rev. Lett.* **2005**, *95* (5), 056105/1–056105/4.

(73) Lagugne-Labarthet, F.; Bruneel, J. L.; Rodriguez, V.; Sourisseau, C. Chromophore Orientations in Surface Relief Gratings with Second-Order Nonlinearity as Studied by Confocal Polarized Raman Microspectrometry. *J. Phys. Chem. B* **2004**, *108* (4), 1267–1278.

(74) Lyulin, A. V.; Li, J.; Mulder, T.; Vorselaars, B.; Michels, M. A. J. Atomistic simulation of bulk mechanics and local dynamics of amorphous polymers. *Macromol. Symp.* **2006**, *237*, 108–118 (Molecular Mobility and Order in Polymer Systems).

(75) Walasek, J. Local order in a globally deformed polymer network with nematiclike interactions. *J. Polym. Sci., Part B: Polym. Phys.* **1990**, *28* (7), 1075–1091.

(76) Yang, S.; Michielsen, S. Determination of the Orientation Parameters and the Raman Tensor of the 998 cm^{-1} Band of Poly(ethylene terephthalate). *Macromolecules* **2002**, *35* (27), 10108–10113.

JP807065A